

1 **Part 2: Quantitative contributions of cyanobacterial alkaline phosphatases to biogeochemical  
2 rates in the subtropical North Atlantic**

3 *Noelle A. Held<sup>1,2,3 \*;\*\*</sup>, Korrina Kunde<sup>4,5, \*\*</sup>, Clare E. Davis<sup>6,†</sup>, Neil J. Wyatt<sup>5</sup>, Elizabeth L. Mann<sup>7</sup>, E.  
4 Malcolm S. Woodward<sup>8</sup>, Matthew McIlvin<sup>1</sup>, Alessandro Tagliabue<sup>6</sup>, Benjamin S. Twining<sup>7</sup>, Claire  
5 Mahaffey<sup>6</sup>, Mak Saito<sup>1</sup>, Maeve C. Lohan<sup>5</sup>*

6

7 <sup>1</sup>Department of Marine Chemistry and Geochemistry, Woods Hole Oceanographic Institution, Woods Hole,  
8 USA

9 <sup>2</sup>Department of Environmental Systems Science, ETH Zürich, Zürich, Switzerland

10 <sup>3</sup>Department of Biological Sciences, Marine and Environmental Biology Section, University of Southern  
11 California, Los Angeles, CA, USA

12 <sup>4</sup>School of Oceanography, University of Washington, Seattle, USA

13 <sup>5</sup>Ocean and Earth Sciences, National Oceanography Centre, University of Southampton, Southampton, UK

14 <sup>6</sup>Department of Earth, Ocean, and Ecological Sciences, University of Liverpool, Liverpool, UK

15 <sup>7</sup>Bigelow Laboratory for Ocean Sciences, East Boothbay, USA

16 <sup>8</sup>Plymouth Marine Laboratory, Plymouth, UK

17

18 \*Corresponding author: N.A. Held (nheld@usc.edu)

19 \*\*These authors contributed equally

20 <sup>†</sup>now at: Springer Nature, London, UK

21 **Abstract**

22 Microbial enzymes alter marine biogeochemical cycles by catalyzing chemical transformations that  
23 bring elements into and out of particulate organic pools. These processes are often studied through  
24 enzyme rate-based estimates and nutrient-amendment bioassays, but these approaches are limited in  
25 their ability to resolve species-level contributions to enzymatic rates. Molecular methods including  
26 proteomics have the potential to link the contributions of specific populations to the overall  
27 community enzymatic rate; this is important because organisms will have distinct enzyme  
28 characteristics, feedbacks, and responses to perturbations. Integrating molecular methods with rate  
29 measurements can be achieved quantitatively through absolute quantitative proteomics. Here, we use  
30 the subtropical North Atlantic as a model system to probe how a combination of traditional bioassays  
31 and absolute quantitative proteomics can provide a more comprehensive understanding of nutrient  
32 limitation in marine environments. The experimental system is characterized by phosphorus stress and  
33 potential metal-phosphorus co-limitation due to dependence of the organic phosphorus scavenging  
34 enzyme alkaline phosphatase on metal cofactors. We performed nutrient amendment incubation  
35 experiments to investigate how alkaline phosphatase absolute abundance and activity is affected by  
36 trace metal additions and develop an inventory of cyanobacterial alkaline phosphatases. We show that

Deleted: <sup>8</sup>

38 the two most abundant picocyanobacteria, *Prochlorococcus* and *Synechococcus* are minor contributors  
39 to total alkaline phosphatase activity as assessed by a widely used enzyme assay, with  
40 *Prochlorococcus* accounting for 3-35% and *Synechococcus* contributing 0.5-5% of alkaline  
41 phosphatase activity depending on location and metal cofactor. This was true even when trace metals  
42 were added, despite both species having the genetic potential to utilize both the Fe and Zn containing  
43 enzymes, PhoX and PhoA respectively. Serendipitously, we also found that the alkaline phosphatases  
44 responded to cobalt additions suggesting possible substitution of the metal center by Co in natural  
45 populations of *Prochlorococcus* (substitution for Fe in PhoX) and *Synechococcus* (substitution for Zn  
46 in PhoA). This integrated approach allows for a nuanced interpretation of how nutrient limitation  
47 affects marine biogeochemical cycles and highlights the benefit of building quantitative connections  
48 between rate and “-omics” based measurements.

49

**Formatted:** Font: Italic

**Formatted:** Font: Italic

**Deleted:** .

51 **Introduction**

52 Microbial enzymes alter marine biogeochemical cycles by catalysing chemical transformations and  
53 facilitating the movement of elements through planetary reservoirs. On one hand, enzyme  
54 contributions from different groups of microbes can be considered collectively, for instance in rate-  
55 based or bioassay incubation experiments where the activities of the entire microbial community are  
56 aggregated. On the other hand, we anticipate that the enzymes of different organisms will have  
57 different activities and responses to perturbations; this means that resolving enzyme provenance could  
58 enhance the quantitative connection between microbial activity and biogeochemical rates (e.g. the  
59 goals of the fledgling Biogeoscapes program (Saito et al., 2024)). “-Omics” based methods,  
60 particularly proteomics which directly resolves protein/enzyme concentrations, can provide a window  
61 into the relationships between microbial abundance, enzyme concentration, and biogeochemical rates.

62 In this work we use quantitative proteomics to constrain the relative contributions of different  
63 microbes (*Synechococcus* and *Prochlorococcus*) to biogeochemical rates of alkaline phosphatase  
64 activity in the oligotrophic subtropical North Atlantic gyre. In this region, primary production is  
65 constrained by availability of dissolved inorganic nitrogen (DIN) and phosphorus (DIP), but inputs of  
66 atmospherically derived iron (Fe) from Saharan desert dust create a niche for nitrogen fixation,  
67 partially alleviating nitrogen limitation but driving the system to DIP depletion (Martiny et al., 2019;  
68 Moore et al., 2013). Lack of DIP then drives a shift towards the acquisition of the abundant yet less  
69 bioavailable dissolved organic phosphorus (DOP) by phytoplankton (Lomas et al., 2010; Mather et al.,  
70 2008). The DOP pool includes relatively labile phosphomono- and diesters (together ~75 to 85 % of  
71 DOP) that derive from ribonucleic acids, adenosine phosphates and phospholipids (Kolowith et al.,  
72 2001; Young and Ingall, 2010). These compounds cannot be directly assimilated but require the  
73 phosphate group to be cleaved from the ester moiety first. Cleaving is catalysed by a range of  
74 hydrolytic enzymes, such as alkaline phosphatases, which are common in marine microbes, including  
75 bacterial as well as eukaryotic phytoplankton (Dyrman and Ruttenberg, 2006; Luo et al., 2009;  
76 Shaked et al., 2006). Reflecting this, alkaline phosphatase activity (APA) is high across the  
77 oligotrophic gyres (Browning et al., 2017; Davis et al., 2019; Duhamel et al., 2010; Mahaffey et al.,  
78 2014; Wurl et al., 2013).

79 Alkaline phosphatase activity is commonly regulated by intracellular phosphate levels  
80 (Santos-Benito, 2015) and appears to be closely linked to low ambient DIP concentrations (Mahaffey  
81 et al., 2014). However, these enzymes also have a metal dependence, as metal co-factors are involved  
82 in the hydrolysis process at the active site. Different alkaline phosphatases exist that, while sharing  
83 function, evolved independently and have distinct metal requirements. For example, in *Escherichia*  
84 *coli* (*E. coli*) the alkaline phosphatase PhoA has two Zn<sup>2+</sup> (zinc) or Co<sup>2+</sup> (cobalt) ions and one Mg<sup>2+</sup>  
85 (magnesium) ion at each active site per homodimer (Coleman, 1992), and in *Pseudomonas fluorescens*

86 the monomeric alkaline phosphatase PhoX has two Fe<sup>3+</sup> ions and three Ca<sup>3+</sup> (calcium) ions(Yong et  
87 al., 2014). The active sites of PhoA and PhoX in marine microbes have yet to be characterized but  
88 based on sequence homology are presumed to be like these model organisms, leading to the  
89 hypothesis that alkaline phosphatase activity to be limited by scarce Fe, Zn, or Co trace metals in the  
90 marine environment (Lohan and Tagliabue, 2018).

91 Global change is predicted to intensify phosphorus stress and alter trace metal and nutrient  
92 cycles in the ocean (Hoffmann et al., 2012; Kim et al., 2014). Throughout the North Atlantic, the  
93 utilisation of DOP is widespread(Mather et al., 2008) and whole community rates of APA are high  
94 compared with other oceanic regions (Duhamel et al., 2010; Mahaffey et al., 2014). At this time, it is  
95 not known which microbes and enzyme types are responsible for bulk APA in the North Atlantic and  
96 elsewhere. Resolving this could lead to a more quantitative understanding of how APA activity is  
97 regulated in the modern ocean, allowing better predictions of future changes in enzyme abundance  
98 and activity and the resulting influence on carbon export. In this study, we use field-based quantitative  
99 proteomics to develop an inventory of alkaline phosphatase activity and to identify nutrient-related  
100 regulatory controls on alkaline phosphatase that are distinct for different organisms. We use this as a  
101 proof of concept for developing quantitative connections between biogeochemical rates and “-omics”  
102 based measurements of microbial enzymes, a topic that is of interest to ongoing international efforts  
103 to characterize ocean metabolism.

## 104 **Methods**

### 105 **Shipboard bioassays**

106 All samples for this study were collected on board the *RRS James Cook* during research cruise JC150  
107 (GEOTRACES process study GApr08), on a zonal transect at 22 °N leaving Guadeloupe on June 26<sup>th</sup>  
108 and arriving in Tenerife on August 12<sup>th</sup>, 2017, with multiple stations occupied for bioassays. A  
109 detailed description of the bioassays and analysis of environmental parameters is presented in  
110 Mahaffey et al. (submitted as a companion to this article).

111 Briefly, surface seawater was collected and processed according to trace metal clean protocols  
112 and before dawn. For each location, duplicate or triplicate 24 L polycarbonate (Nalgene) carboys were  
113 filled and spiked with additions of Fe, Zn or Co, as detailed in Table 1. The seawater was incubated at  
114 ambient sea surface temperature and 50 % surface light level for 48 h from dawn to dawn with a  
115 12:12 h simulated light cycle using white daylight LED panels.

116 *Table 1 Bioassay details at each station, showing the types of treatments, the amount of metal added, and the number of*  
117 *replicates per treatment for which proteomics analyses were conducted. Note that one of the three replicates of the Fe*  
118 *addition at the Station at 31 °W (\*) was removed as an outlier from all further analysis.*

	Station at 54 °W	Station at 50 °W	Station at 45 °W	Station at 31 °W
--	------------------	------------------	------------------	------------------

Treatment	Control	-	-	-	-
Fe	+ 1.0 nM	+ 1.0 nM	+ 1.0 nM	+ 1.0 nM	
Zn	+ 1.0 nM	+ 1.0 nM	+ 0.5 nM	+ 1.0 nM	
Co	+ 50 pM	+ 50 pM	+ 50 pM	+ 20 pM	
Replicates per treatment	2	2	2	3*	

119 After the incubation period, subsamples for proteins were collected into acid cleaned 10 L  
 120 polycarbonate carboys (Nalgene) and immediately filtered, collecting the >0.22 µm fraction on  
 121 polyethersulfone membrane filter cartridges (Millipore, Sterivex) and recording the filtered volume.  
 122 Any remaining water was pressed out with an air-filled syringe, the filtration unit was sealed with clay  
 123 and then frozen at -80 °C. This procedure was repeated for the second (and third where applicable)  
 124 replicate of each treatment.

125 **Alkaline phosphatase activity (APA) rate measurements**

Formatted: Font: Bold

126 Total APA was measured in unfiltered seawater samples using the synthetic fluorogenic  
 127 substrate 4- methylumbelliferyl-phosphate (MUF, Sigma Aldrich, Ammerman 1993, Davis et al  
 128 2019). MUF stock solutions (100 nM in 2-methoxyethanol) were diluted with Milli-Q deionized  
 129 water (200 µM stock). Unfiltered seawater was spiked with the MUF substrate to final  
 130 concentrations of 500 nM or 2000 nM MUF for single substrate additions, or a series of replicates  
 131 were incubated over a final MUF concentration range from 100 nM to 2000 nM for the  
 132 determination of enzyme kinetic parameters, Vmax and Km. Once spiked, samples were incubated in  
 133 polycarbonate bottles in triplicate in the temperature and light adjusted reefer container for up to 12  
 134 hours.

Formatted: Font: 11 pt

Formatted: Line spacing: 1.5 lines

135 MUF hydrolysis to the fluorescent product, 4- methylumbellifrone (MUF), was  
 136 measured at regular intervals (typically every 90 minutes) over a period of up to 8 - 12 hours using a  
 137 Turner 10Au field fluorometer (365 nm excitation, 455 nm emission) after the addition of a buffer  
 138 solution (3 : 1 sample: 50 mM sodium tetraborate solution, pH 10.5). A calibration was produced at  
 139 the start and end of the cruise using MUF standards (concentration range 0–1000 nM) to ensure  
 140 linearity of the fluorescence of MUF over the expected concentration range. Fluorescence response  
 141 factors were determined daily using freshly prepared 200 nM MUF stocks and was used to convert the  
 142 rate of change in fluorescence to MUF hydrolysis rate, here considered to be synonymous with  
 143 volumetric APA (nM P h<sup>-1</sup>). Boiled seawater blanks (500 nM MUF) were incubated in parallel with  
 144 samples to ensure that there was no significant change in fluorescence due to abiotic degradation or  
 145 hydrolysis over time. Enzyme kinetic parameters were determined using a range of MUF  
 146 concentrations. Michaelis-Menten equation was transformed to produce substrate-response curves or  
 147 linear regression plots and the maximum hydrolysis rates (Vmax) and half saturation constant (Km)

Formatted: Indent: First line: 0.5", Line spacing: 1.5 lines

Formatted: Line spacing: 1.5 lines

Formatted: Font: 11 pt

148 were determined using the Hanes-Woolf plot graphical linearization of the Michaelis-Menten  
149 equation following Duhamel et al., 2011.

150  
151 **Protein extraction and digestion**

152 All plastics materials were washed with ethanol and dried before usage. All samples from one station  
153 were processed together in one extraction and digestion cycle. The frozen Sterivex filter cartridges  
154 were transported to the laboratory on ice and cut open with a tube cutter. The filters were cut out from  
155 their holders with razor blades and placed into 2 ml microfuge tubes (Eppendorf). Following  
156 previously established protocols(Held et al., 2020; Saito et al., 2014)Click or tap here to enter text.,  
157 proteins were extracted in a 1 % sodium dodecyl sulfate (SDS) buffer for 15 min at 20 °C, followed  
158 by 10 min at 95 °C for denaturation, and 1 h at 20 °C while shaking at 350 rpm. The protein extract  
159 was then centrifuged at 13.5 rpm for 20 min, with the impurities-free supernatant collected and then  
160 spin-concentrated for 1 h in 5 kD membrane filters (Vivaspin, GE Healthcare). Total protein  
161 concentrations were then measured by bicinchoninic assay (BCA) (Pierce) on a Nanodrop ND-1000  
162 spectrophotometer (ThermoScientific). Proteins were left to precipitate in a 50:50 solvent mixture of  
163 methanol and acetone (Fisher) with 0.004 % concentrated HCl (Sigma, ACS 37 %) for 5 days at -20  
164 °C. At the end of the precipitation period, samples were centrifuged at 13.5 rpm at 4 °C, supernatants  
165 were removed, and the remaining protein pellets were vacuum-dried (DNA110 Savan SpeedVac,  
166 ThermoFisher). Pellets were redissolved in 50 µl SDS buffer, and the post-precipitation total protein  
167 concentrations were measured via a second BCA assay to assess recovery. The protein extracts were  
168 digested with the proteolytic enzyme trypsin (1 µg per 20 µg protein; Promega #V5280) in a  
169 polyacrylamide tube gel(Lu and Zhu, 2005). The digested samples were concentrated by vacuum  
170 drying and stored at -20 °C until analysis. The final volume was recorded to calculate the total protein  
171 concentration in the processed sample, typically ~1 µg µl<sup>-1</sup>.

172 **Target protein selection**

173 Protein biomarkers for *Synechococcus* and *Prochlorococcus* were chosen to detect DIP stress (PstS)  
174 and related coping mechanisms via DOP hydrolysis (PhoA and PhoX) in our samples (Table 2). PstS  
175 is the substrate-binding protein of the high-affinity phosphate ABC (ATP-Binding Cassette)  
176 transporter, which is upregulated under low intracellular phosphate concentrations via the *pho* regulon  
177 and has previously been used as an indicator of DIP stress (Cox and Saito, 2013; Martiny et al., 2006;  
178 Scanlan et al., 1993). PhoA and PhoX are the Zn/Co-dependent and Fe-dependent alkaline  
179 phosphatases, respectively, which facilitate the acquisition of phosphorus from the DOP pool.

180 *Table 2 Details on the quantified peptide biomarkers that are used to represent each protein in the subsequent plots and*  
181 *discussions. For Prochlorococcus strains, 'HL' and 'LL' refer to high-light and low-light adapted strains, respectively.*

Protein	Quantified peptide (amino acid sequence)	Isolate strains with this peptide
---------	---	-----------------------------------

**Deleted:** (

**Deleted:** )

**Formatted:** Font: 11 pt

**Formatted:** Font: 11 pt

**Formatted:** Font color: Custom Color(RGB(20,18,19))

**Formatted:** p1, Indent: First line: 0", Space Before: 0 pt, After: 0 pt, Line spacing: single

**Deleted:** Table 2

**Formatted:** Font: (Default) Times New Roman

<i>Synechococcus</i>	<b>PhoA</b>	HYIAVALER	WH8102 (clade III)
	<b>PhoX</b>	SQAGAELFR	WH8102 (clade III)
	<b>PstS</b>	WFQELAAAGGPK	RCC307 (clade X)
<i>Prochlorococcus</i>	<b>PhoA</b>	IYVIDPSSSPALLER	MIT9311 (clade HL II) MIT9312 (clade HL II) MIT9314 (clade HL II)
	<b>PhoX</b>	GNLWIQTDGK	MIT9314 (clade HL II)
	<b>PstS</b>	LSGAGASFPK	MIT9301 (clade HL II) MIT9302 (clade HL II) MIT9311 (clade HL II) MIT9312 (clade HL II) MIT9314 (clade HL II) SB (clade HL II) NATL1A (clade LL I) NATL2A (clade LL I)

185

186 The criteria for a peptide of the protein biomarker to be used for quantification were as  
 187 follows. Firstly, we attempted to minimise the presence of methionine and cysteines because they are  
 188 subject to oxidation and cause modifications of the mass-to-charge ratio ( $m/z$ ) during the analyses.  
 189 Secondly, the specificity and least common ancestor of each tryptic peptide was assessed using  
 190 METATRYP (<https://metatryp.whoi.edu/>) (Saunders et al., 2020). It has been demonstrated that  
 191 carefully selected tryptic peptides, screened by using tryptic peptides databases made from genome  
 192 sequences like METATRYP, can be used to identify specific proteins in mixed microbial assemblages  
 193 to the species or even sub-species (ecotype) taxonomic resolution (Saito et al., 2015). Finally, the  
 194 performance of each precursor ion was visually inspected in Skyline (MacLean et al., 2010) for peak  
 195 shape and signal to noise-ratio during uncalibrated test measurements using a target list containing  
 196 many peptides of cyanobacterial alkaline phosphatases on a subset of the incubation samples.

197 **Isotopically labelled standard peptides**

198 The absolute quantitation of the target peptides was achieved using heavy nitrogen isotope-labelled  
 199 peptide standards (Saito et al., 2020). Briefly, DNA was synthesized containing the reverse-translated  
 200 gene sequences for our target peptides interspaced with spacer sequences and ligated with a  
 201 PET30a(+) plasmid vector using the BAMHI 5' and XhoI 3' restriction sites (Novagen; obtained  
 202 through PriorityGENE, Genewiz). Different nucleotide sequences were used to encode for the spacer  
 203 (amino acid sequence: TPELFR) to avoid repetition. As per manufacturer instructions, the plasmid  
 204 was suspended in TE buffer (10 mM Tris-HCl, 1 mM ethylenediaminetetraacetic acid) to 10 ng  $\mu$ l<sup>-1</sup>  
 205 and of this 1  $\mu$ l was added to 20  $\mu$ l competent Tuner(DE3)pLysS *E. coli* cells on ice. The cells were  
 206 heated to 42 °C for 30 sec to initiate transformation, followed by 2 min on ice. At room temperature,  
 207 80  $\mu$ l <sup>15</sup>N-enriched (98 %, Cambridge Isotope Laboratories), kanamycin-containing (50  $\mu$ g ml<sup>-1</sup>) SOC  
 208 medium was added, and cells were incubated for 30 min at 37 °C at 300 rpm. Subsequently, 25  $\mu$ l  
 209 were transferred to pre-heated (37 °C) 50  $\mu$ g ml<sup>-1</sup> agar plates and incubated overnight. One colony was

210 added to 500  $\mu\text{l}$   $^{15}\text{N}$ -enriched SOC medium containing 50  $\mu\text{l ml}^{-1}$  kanamycin as a starter culture and  
211 incubated for 3 h at 37 °C at 350 rpm. Next, 200  $\mu\text{l}$  of the starter culture were transferred into 50 ml  
212 flat incubation flasks with 10 ml SOC medium and incubated for approximately 3 h at 37 °C and 350  
213 rpm until the optical density at 600 nm reached 0.6. Protein production was induced by the addition of  
214 100 mM isopropyl  $\beta$ -D-1-thiogalactopyranoside to the culture and incubating at 25 °C overnight.  
215 Inclusion bodies were initially harvested using BugBuster protein extraction protocols (Novagen).  
216 The remaining pellet containing the inclusion bodies, i.e. the insoluble protein fraction, was  
217 resuspended in 400  $\mu\text{l}$  6 M urea, left on the shaker table at 350 rpm at room temperature for 3 h, and  
218 then moved to the fridge overnight. The next morning, the proteins were reduced, alkylated, and  
219 digested with trypsin as outlined above for the bioassay samples, and stored frozen at -20 °C until use.

220 **Absolute protein quantitation**

221 To determine the absolute concentration of the peptides in the heavy peptide mixture, commercial  
222 standard peptides of known concentration were used. In addition to the peptides of interest, a range of  
223 tryptic peptide sequences from commercially available standards (apomyoglobin, Sigma; Pierce  
224 Bovine Serum Albumin, ThermoFisher) were included in the original plasmid design. Using these, the  
225 calibrated concentration of the heavy peptide mixture had a relative standard deviation of 57 %, with  
226 the standard deviation resulting from the cross-peptide and cross-replicate variability (n=3) (Fig. S1).  
227 A systematic method-focused study addressing the precision and accuracy of these measurements as  
228 well as the development of reference materials will be essential for using absolute quantitative  
229 proteomics in the marine environment in the future (Saito et al., 2024). The linear performance range  
230 of each heavy peptide standard was assessed using standard curves of the peptide mixture. Targeted  
231 proteomic measurements were made by high pressure liquid chromatography with tandem mass  
232 spectrometry (HPLC-MS/MS) on an Orbitrap Fusion Tribrid Mass Spectrometer (ThermoFisher).  
233 Two  $\mu\text{g}$  of each sample diluted to 10  $\mu\text{l}$  in buffer B (0.1 % formic acid in acetonitrile) was spiked with  
234 10 fmol  $\mu\text{L}^{-1}$  of the heavy peptide mixture and injected into the Dionex nanospray HPLC system at a  
235 flow rate of 0.17  $\mu\text{l min}^{-1}$ . The chromatography consisted of a nonlinear gradient from 5 to 95 % of  
236 buffer B with the remaining concentration consisting of buffer A (0.1 % formic acid in LC-grade  
237  $\text{H}_2\text{O}$ ). Precursor ( $\text{MS}^1$ ) ions were scanned for the  $\text{m/z}$  of the heavy peptide standards and their natural  
238 light counterparts. The mass spectrometer was run in parallel reaction monitoring mode and only  
239 peptides included in the precursor inclusion list were selected for fragmentation. Absolute peptide  
240 concentrations were calculated from the ratio of the peak areas of the product ions ( $\text{MS}^2$ ) of the heavy  
241 peptide of known concentration to the natural light peptide (calculated in Skyline (MacLean et al.,  
242 2010)). Manual validation of peak shapes was performed for each peptide and sample. Differences  
243 between samples with regards to filtration volume, initial protein mass and recovery after  
244 precipitation were accounted for. Final peptide concentrations will hereafter be used to represent  
245 corresponding protein concentrations, with the caveat that the measurements are not able to discern

**Deleted:** 5

**Deleted:** Due to the lack of reference materials, the accuracy of the protein concentrations in our bioassay samples cannot be assessed.

250 active versus non-active proteins. The status of metalation and if the protein is correctly folded or  
251 functions as a polymeric complex cannot be determined from this method.

252 **Identification of significant responses to metal additions**

**Deleted:** S

253 Changes in protein concentrations in response to metal additions were compared relative to the  
254 unamended control treatment after 48 h. This approach accounts for any bottle effects. Due to the  
255 unique challenges of ocean proteomics sampling and large-scale trace-metal clean bioassays, treatment  
256 replication was limited to  $n = 2$  at 54 °W, 50 °W and 45 °W and to  $n = 3$  at 31 °W. Many statistical  
257 tests assume normal distributions, which for  $n = 2$  is not assessable. Therefore, in our case, significant  
258 differences in protein concentrations were evaluated using a two-fold change criterion, in which the  
259 concentrations in all replicates of the metal treatments must lie outside a two-fold change in the  
260 average  $\pm$  one standard deviation of the control to be deemed a significant response. The fold-change  
261 in expression and in particular the two-fold change is ~~a commonly used metric to identify proteins that~~  
262 are significantly more or less expressed across different conditions (Carvalho et al., 2008; Lundgren et  
263 al., 2010; Zhang et al., 2006).

**Deleted:** an accepted and

264 For the biogeochemical parameters measured in the bioassays, i.e. Chl-*a*, APA and cell counts  
265 replication was not limited to  $n=2$  in most cases. Where  $n=3$ , ANOVA ( $\alpha=0.05$ ) followed by Tukey  
266 posthoc tests were applied to compare the Control treatments with other treatments.

267 **Results and Discussion**

268 **Biogeochemical setting**

269 The oligotrophic subtropical North Atlantic is marked by high deposition of Saharan desert dust,  
270 delivering large amounts of Fe and other lithogenic trace metals to the surface ocean (Kunde et al.,  
271 2019). During JC150, contrasting biogeochemical regimes existed in the western and eastern basin  
272 with high-metal, low-phosphorus, low-nitrogen surface waters at the 54 °W and lower-metal, higher-  
273 phosphorus, higher-nitrogen surface waters 31 °W (Mahaffey et al. (2025; companion article)).  
274 Furthermore, *Synechococcus* was two-fold more abundant in the west than in the east, whilst  
275 *Prochlorococcus* was more than six-fold more abundant in the east than in the west and numerically  
276 more abundant than *Synechococcus* throughout. Overall, the stations at 50 °W and 45 °W exhibited  
277 biogeochemical intermediates to the conditions in the east and west. The confluence of gradients in  
278 both DIP and trace element availability, as well as clear shifts in microbial community structure,  
279 provide a natural field laboratory to probe how environmental drivers differentially influence the  
280 contributions of dominant microbes to whole-ecosystem enzyme activity.

**Deleted:** submitted as a companion to this article

281 *Table 3 Date, location and biogeochemical conditions at 40 m depth at the start ( $t_0$ ) of the bioassays. Biogeochemical*  
282 *parameters are presented as the average  $\pm$  one standard deviation of replicate  $t_0$  samples, except for the singlet samples of*

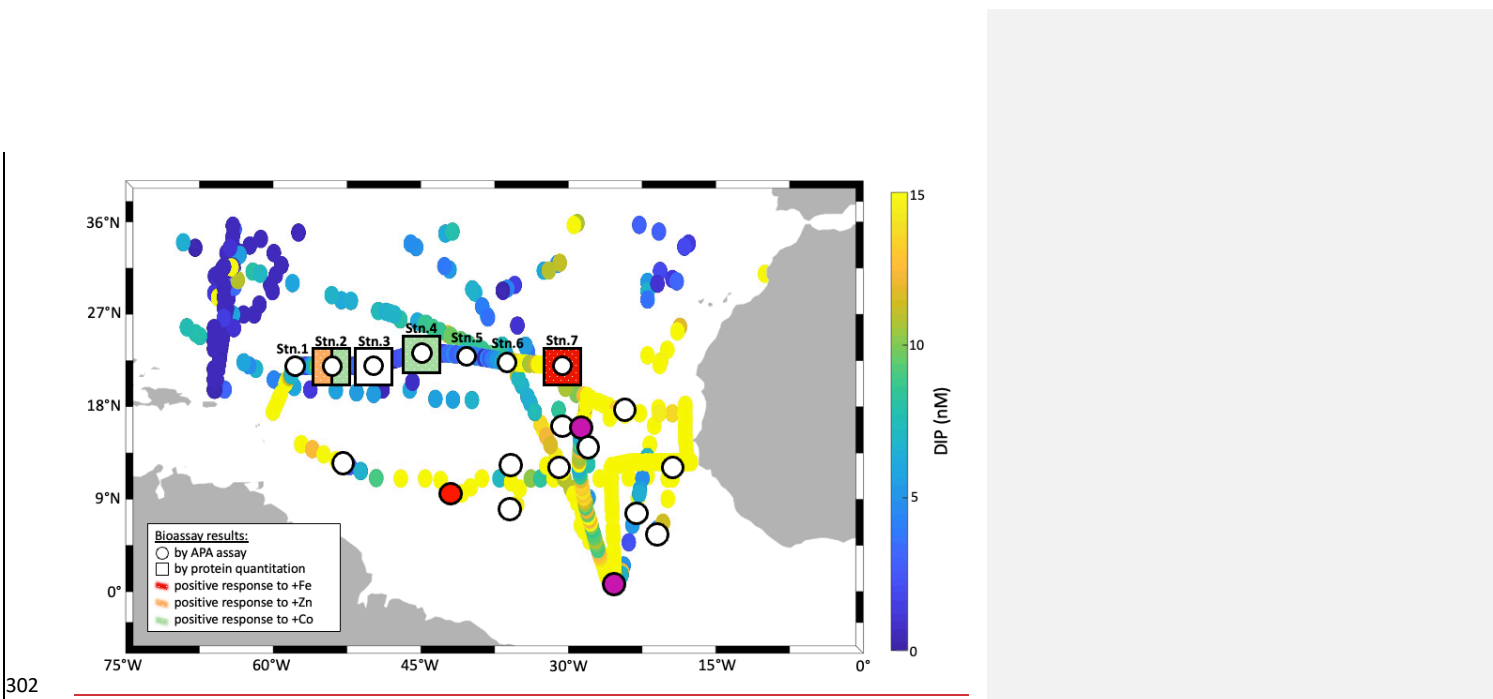
286 DOP at Station 4 and dCo at all stations. Mixed layer depths (MLD; defined after <sup>52</sup>) averages over multiple days, as these  
 287 were not always determined on the exact day of bioassay set-up.

	Parameter	Station at 54 °W	Station at 50 °W	Station at 45 °W	Station at 31 °W
General	Date	11 <sup>th</sup> July 2017	15 <sup>th</sup> July 2017	19 <sup>th</sup> July 2017	5 <sup>th</sup> August 2017
	Location	22 °N 54 °W	22 °N 50 °W	23 °N 45 °W	22 °N 31 °W
	SST (°C)	27	27	26	25
	MLD (m)	24 ± 3 (5 <sup>th</sup> to 8 <sup>th</sup> July)	33 ± 1 (12 <sup>th</sup> to 15 <sup>th</sup> July)	42 ± 9 (17 <sup>th</sup> to 20 <sup>th</sup> July)	51 ± 8 (4 <sup>th</sup> to 8 <sup>th</sup> August)
Macronutrients	DIP (nM)	3.7 ± 2.1	3.7 ± 1.0	3.4 ± 0.8	14 ± 0.70
	DOP (nM)	87 ± 7.5	137 ± 39	112	129 ± 29
	DIN (nM)	1.5 ± 1.9	1.66 ± 0.56	3.36 ± 1.0	6.2 ± 0.0
	APA (nM h <sup>-1</sup> )	2.8 ± 0.21	2.86	2.48 ± 0.10	1.15 ± 0.08
Trace metals	dFe (nM)	1.26 ± 0.06	0.53 ± 0.06	0.83 ± 0.00	0.23 ± 0.05
	dZn (nM)	0.25 ± 0.14	0.46 ± 0.09	0.14 ± 0.01	0.04 ± 0.01
	dCo (pM)	11.0	11.1	13.0	13.9
Phytoplankton community	<i>Synechococcus</i> (cells ml <sup>-1</sup> )	3.4 ± 0.55 · 10 <sup>3</sup>	-	-	1.6 ± 0.26 · 10 <sup>3</sup>
	<i>Prochlorococcus</i> (cells ml <sup>-1</sup> )	29 ± 0.37 · 10 <sup>4</sup>	-	-	181 ± 0.37 · 10 <sup>4</sup>
	Chl- <i>a</i> (µg L <sup>-1</sup> )	0.064 ± 0.01	0.055 ± 0.01	0.110 ± 0.06	0.149 ± 0.005

288

#### 289 Alkaline phosphatase responded differently in the traditional vs proteomic bioassays

290 We measured responses in alkaline phosphatase activity (traditional bioassay) and enzyme identity  
 291 and provenance (proteomic assay) to metal additions across the North Atlantic gyre. Both assays were  
 292 performed on matched samples at four locations (St 2, 3, 4, 7; Figure 1), allowing direct comparison  
 293 of the results. In all cases for the traditional assay (shown as circles in Figure 1), bulk alkaline  
 294 phosphatase activity did not increase significantly upon metal additions (see also Figure 2). However,  
 295 the proteomic assay revealed that specific alkaline phosphatases did respond positively to the metal  
 296 additions (squares in Figure 1), depending on the location and metal added. The discrepancy between  
 297 the traditional bioassay (no response) and proteomic assay (specific, albeit patchy responses) merited  
 298 additional exploration of the two approaches, which we detail below. One important explanation  
 299 emerges from the fact that the APA assay covers the entire microbial community (i.e. everything from  
 300 bacteria to eukaryotes) but the proteomics measurements are specific to a subset of *Prochlorococcus*  
 301 and *Synechococcus*.



302

303 **Figure 1** Summary of traditional and molecular bioassay results from this manuscript and others. Map of the North Atlantic  
 304 showing surface phosphate concentrations (compiled by Martiny *et al.*, 2019 and augmented with data from Browning *et al.*  
 305 2017. Overlain are locations of bioassays, where the response of APA to metal additions was tested (circles), and of  
 306 bioassays, where the absolute concentration of the alkaline phosphatase proteins was measured in response to metal  
 307 additions (squares). Bioassays of the present study include longitudinal station labels. The others are from Mahaffey *et al.*  
 308 (2014) and Browning *et al.* (2017) as well as from additional bioassays during JC150 Mahaffey *et al.* (submitted as a  
 309 companion to this article), but where no protein measurements were made. Symbols at bioassay locations are coloured in  
 310 orange, green or red, if a positive response was observed upon addition of Fe, Zn or Co respectively.

311 **Variability in the response to metal additions in the traditional bioassays**

312 As mentioned above, there was no significant response in bulk alkaline phosphatase activity  
 313 to metal additions at any of the stations. Here we focus on Stations 2, 3, 4, and 7, where matched  
 314 proteomic assays were also conducted. However, alkaline phosphatase assays were conducted on  
 315 incubations at all seven stations, and there was no response to metal addition at any of them, nor in  
 316 APA rates normalized to chl-a (Figures S2-S5 and see Table S6). Given this, we sought to address  
 317 whether there were other observable shifts in microbial activity as a result of the metal additions,  
 318 including in Chl-A (a proxy for phytoplankton growth) and cell counts for *Prochlorococcus* and  
 319 *Synechococcus* (Figure 2). While there were no statistically significant changes, either positive or  
 320 negative, in any of these conventional assays, there were differences between replicate incubation  
 321 bottles and within the basal conditions across the stations. Despite our efforts to homogenize the  
 322 incubations and work in large volumes, this variation seems to result from stochasticity of sampling  
 323 the low biomass system of the subtropical North Atlantic gyre, particularly since there is clear  
 324 variation among the control bottles as well as in the amended conditions. It is also consistent with past  
 325 literature including Browning *et al.*, 2017 in which only one in eight experiments showed a metal  
 326 driven response in APA and Mahaffey *et al.*, 2014 in which there was a positive response of APA to

**Commented [NH1]:** The colors in this figure are now color blind safe

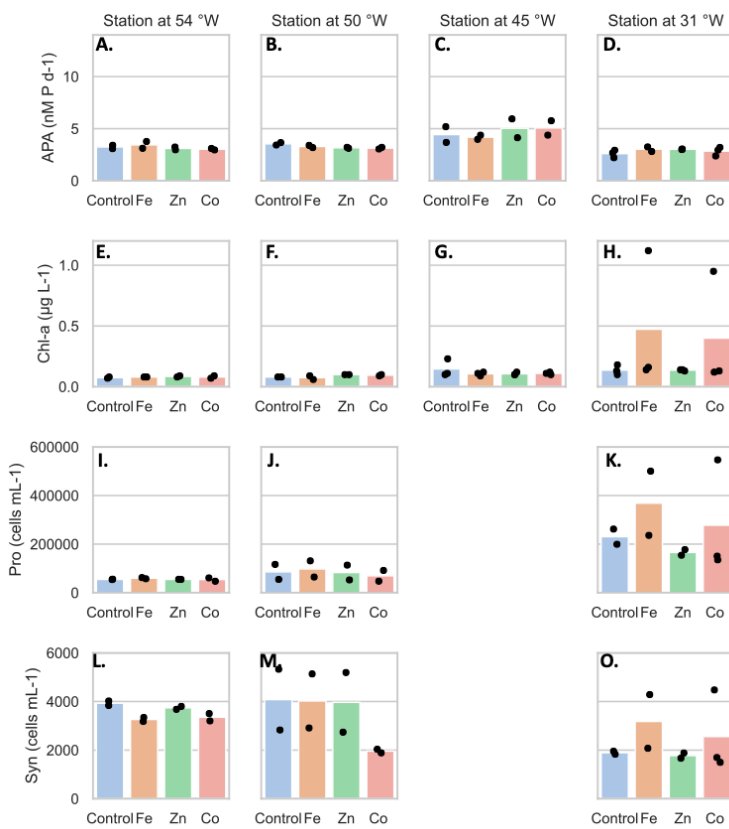
**Formatted:** Indent: First line: 0.5", Don't keep with next

**Formatted:** Font: Italic

**Formatted:** Font: Italic

**Formatted:** Font: Not Italic

327 Zn only in the eastern basin (see Figure 1). One possible explanation for the presence of the many null  
 328 responses across the basin is that organisms could be re-allocating metals towards use in alkaline  
 329 phosphatases when under phosphorus stress. Supporting this idea, a comparable re-allocation  
 330 mechanism of cellular Fe between metalloproteins involved in biological N<sub>2</sub> fixation and  
 331 photosynthesis has previously been demonstrated in the diel cycle of *Crocospaera watsonii* (Saito et  
 332 al., 2011b). Regardless, the absence of significant responses in the biogeochemical parameters  
 333 contrasted notably with the observed responses in protein data detailed below.



Formatted: Centered

334

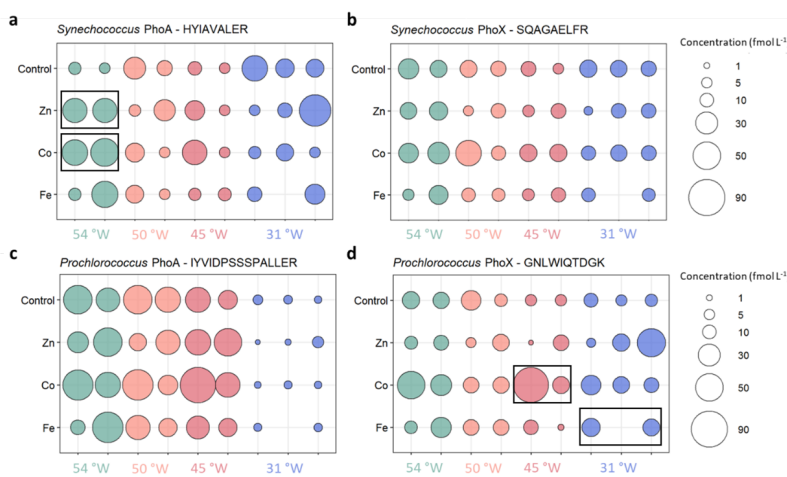
335 Figure 2. Mean concentrations (bars) of the bioassay parameters after the addition of Fe, Zn and Co at the four stations,  
 336 specifically concentrations of chlorophyll a (µg L<sup>-1</sup>), (A-D) rates of alkaline phosphatase (nM d<sup>-1</sup>), (E-H) Prochlorococcus  
 337 abundance (cells mL<sup>-1</sup>) (I-K) and Synechococcus abundance (cells mL<sup>-1</sup>) (L-O). Dots represent the concentrations of each  
 338 replicate. Note the data gap for cell counts at the Station at 45°W.

339 Strain-resolved cyanobacterial alkaline phosphatases did respond to metal additions

340 In contrast to the bioassay results, there were clear changes in proteomically-resolved alkaline  
 341 phosphatase concentrations after metal additions. We focused on the enzymes PhoA and PhoX and

Commented [NH2]: This figure has been replotted for clarity

342 used peptides that were specific to one or more strains of either *Prochlorococcus* or *Synechococcus* (343 2) and represent a subset of the population of alkaline phosphatase enzymes in the ocean. We note 344 that marine alkaline phosphatases are found at different subcellular localizations and are also known 345 to be secreted to the environment (i.e. into the dissolved phase) (Li et al., 1998; Luo et al., 2009). Our 346 measurements focus on the alkaline phosphatase associated with microbial cells (i.e. the particulate 347 phase). Coming from an overview of the enzyme concentrations across isoforms, taxa and bioassays, 348 we will discuss how these compare to the APA assay involving fluorogenic substrates.



349

350 *Figure 3* Absolute concentrations of the alkaline phosphatases PhoA (left column) and PhoX (right column) of  
351 *Synechococcus* (top) and *Prochlorococcus* (bottom) in the different metal treatments or the unamended control at the four  
352 probed stations. Bubbles of the same colour are replicates of the same treatment and show the concentrations as fmol  
353 enzyme per L seawater. Black boxes indicate significant change from Control treatment.

354 The results of all measured alkaline phosphatase concentrations are shown in Fig. 3 and all  
355 data is compiled in Table S5. *Synechococcus* PhoA and PhoX concentrations in the control treatments  
356 ranged from 6 to 43 fmol L⁻¹ and 6 to 26 fmol L⁻¹, respectively, with no clear cross-basin trend despite  
357 a strong west-to-east decreasing gradient in *Synechococcus* cell abundance (Table 3). Similarly,  
358 *Prochlorococcus* PhoA and PhoX concentrations in the control treatments ranged from 2 to 55 fmol  
359 L⁻¹ and 6 to 23 fmol L⁻¹, respectively, but with elevated PhoA at in the west and the lowest  
360 concentrations at 31°W, which is opposite to the west-to-east increasing gradient in *Prochlorococcus*  
361 cell abundance. This suggests that we observed a gradient in DIP/trace metal nutrient stress for  
362 *Prochlorococcus*, but not for *Synechococcus*.

363 Our measured alkaline phosphatase concentrations were similar, albeit at the lower end, to  
364 concentrations reported for other cyanobacterial enzymes and nutrient regulators from the North  
365 Pacific (~10⁻¹ to 10³ fmol L⁻¹) (Saito et al., 2014). Interestingly, our alkaline phosphatase

366 concentrations occurred at the same concentration range as other macronutrient stress indicators  
367 (response regulator protein PhoP, sulfolipid biosynthesis protein SqdB, nitrogen regulatory protein P-  
368 II), all of which did not exceed tens of fmol L<sup>-1</sup> (Saito et al., 2014). In contrast, concentrations of the  
369 *Prochlorococcus* PstS transporter protein were higher, ranging from 95 to 472 fmol L<sup>-1</sup> (Table S5).  
370 This is within the concentration range of other cyanobacterial nutrient transporters, such as the urea  
371 transporter UrtA, measured previously (Saito et al., 2014). In mediating nutrient stress, particularly  
372 phosphorus stress, the relative role of transporter proteins (such as PstS) versus other strategically  
373 deployed enzymes like alkaline phosphatase in the oligotrophic specialists *Synechococcus* and  
374 *Prochlorococcus*, represents an interesting avenue for future research.

375 **Evidence for direct biochemical regulation of certain alkaline phosphatases by metals**

Deleted: ¶

... [1]

376 Our strain-specific, quantitative proteomics approach allowed us to resolve contrasting responses  
377 across the sites. The responses differed with varying phytoplankton species, alkaline phosphatase  
378 form and stimulating metal addition, consistent with differences in the biogeochemical regimes (Table  
379 3). At the iron-rich westernmost station (Station 4; 54 °W), the *Synechococcus* PhoA concentration  
380 increased six- and seven-fold upon addition of Zn (to  $38 \pm 0.56$  fmol L<sup>-1</sup>) and Co (to  $47 \pm 6.8$  fmol L<sup>-1</sup>)  
381 relative to the control ( $6.7 \pm 1.5$  fmol L<sup>-1</sup>), respectively. At one intermediate Station (45 °W), the  
382 *Prochlorococcus* PhoX concentration increased 8-fold upon addition of Co relative to the control.  
383 Notably, a direct response of alkaline phosphatase to an addition of Co has not been shown in the field  
384 before. In contrast, at the low iron easternmost station, the *Prochlorococcus* PhoX increased over two-  
385 fold upon Fe addition (to  $18 \pm 2.6$  fmol L<sup>-1</sup>) relative to the control ( $8.2 \pm 2.4$  fmol L<sup>-1</sup>).

Formatted: Font: 12 pt, Not Bold

386 At least three scenarios are possible to explain the increased alkaline phosphatase  
387 concentrations of *Synechococcus* and *Prochlorococcus* in seawater in these treatments – two  
388 biochemical and one growth driven hypotheses. First, the metal addition may stimulate the production  
389 of the alkaline phosphatase enzyme via a direct or indirect metal regulation on the expression of this  
390 enzyme, as was previously observed for PhoA with Zn additions in *Synechococcus* cultures (Cox and  
391 Saito, 2013). Second, the metal addition may prevent the degradation of the existing alkaline  
392 phosphatases by filling empty metal co-factor sites (Bicknell et al., 1985), with the caveat that PhoA  
393 is likely to be periplasmic and hence unlikely to be actively degraded (Luo et al., 2009). Both  
394 biochemical scenarios allow for increased alkaline phosphatase concentrations at a constant cell  
395 abundance. The third explanation is that the alkaline phosphatase concentration increases because the  
396 metal addition stimulates overall cell growth, resulting in higher phosphorus demands and hence more  
397 production of alkaline phosphatase proteins by the cell. This could manifest itself as higher cell  
398 abundances in addition to increased alkaline phosphatase concentration per unit biomass.

399 While the different scenarios are not mutually exclusive, our quantitative proteomic approach  
400 allowed us to discern between biochemical and growth mechanisms by normalising the alkaline

414 phosphatase concentrations to the total cell counts of *Prochlorococcus* and *Synechococcus*, caveating  
415 that the cell counts are not strain-specific, unlike the peptide-based protein measurements. Cell counts  
416 did not change significantly across these treatments Mahaffey et al. (submitted as a companion to this  
417 article), which means that the trends of increased alkaline phosphatase concentration per L seawater  
418 persisted in bioassays (i.e. +Zn and +Co at 54 °W and +Fe at 31 °W; cell counts do not exist for 45  
419 °W) even when converted to the number of alkaline phosphatase enzymes per cell, indicating  
420 biochemical regulation as opposed to simply growth of the responsible organism. Specifically, the  
421 concentration of *Synechococcus* PhoA increased to  $8418 \pm 673$  enzymes cell<sup>-1</sup> upon Co addition and  
422 to  $6057 \pm 48$  enzymes cell<sup>-1</sup> upon Zn addition relative to  $1025 \pm 257$  enzymes cell<sup>-1</sup> in the control at  
423 54 °W, while the concentration of the *Prochlorococcus* PhoX increased to 59 enzymes cell<sup>-1</sup> upon Fe  
424 addition relative to  $19 \pm 7$  enzymes cell<sup>-1</sup> in the control at 31 °W. Therefore, a direct biochemical  
425 metal control on the alkaline phosphatase concentrations during the bioassays is plausible (i.e. either  
426 of the first two explanations) and adds weight to the hypothesis for the localised metal-phosphorus co-  
427 limitation in the subtropical North Atlantic (Browning et al., 2017; Jakuba, R. Wisniewski et al.,  
428 2008; Mahaffey et al., 2014; Saito et al., 2017; Shaked et al., 2006).

429 These estimates of enzyme copies per cell are potentially underestimates as multiple  
430 *Prochlorococcus* and *Synechococcus* ecotypes co-exist and the alkaline phosphatase peptide  
431 sequences probed here do not encompass all of them (Table 2). Moreover, it is also possible that there  
432 are additional isoforms of alkaline phosphatase present in these organisms that have yet to be  
433 identified (Bradshaw et al., 1981). Yet in these marine cyanobacteria, the cellular concentration of  
434 alkaline phosphatase was much higher compared to a measurement in the model bacterium *E. coli*,  
435 which contained  $\sim 4$  PhoA copies cell<sup>-1</sup> (Wiśniewski and Rakus, 2014). This underscores the  
436 ecological demand for alkaline phosphatases due to the significant depletion of phosphorus in the  
437 marine environment. It is yet to be determined whether the per-cell estimates of alkaline phosphatases  
438 presented here are the norm for marine cyanobacteria, or whether these estimates are exceptionally  
439 high due to the prevalence of phosphorus stress in our study region.

440 While PhoX enzymes are unknown to use Co as a metal co-factor and the response at 45 °W  
441 warrants further investigation, the substitution of Zn with Co in PhoA has been hypothesised  
442 previously based on the distributions of trace metals and phosphate in the Sargasso Sea (Jakuba, R.  
443 Wisniewski et al., 2008; Saito et al., 2017). The results from 54 °W support this hypothesis as the  
444 addition of both Zn and Co were associated with almost equal increases of the *Synechococcus* PhoA  
445 concentration relative to the control. It is thought that while Zn is the preferred metal centre for PhoA,  
446 it is possible to substitute Co for Zn in the protein, such as occurs in *Thermotoga maritima*  
447 (Wojciechowski et al., n.d.) *in vivo* and *in vitro* in *E. coli* (Gottesman et al., 1969). Metabolic  
448 substitution capabilities between Zn and Co in carbonic anhydrases have previously been identified in  
449 marine phytoplankton, with similar or slightly reduced growth rates for a range of marine diatoms and

450 coccolithophores, when Zn was replaced with Co in carbonic anhydrases (Dupont et al., 2006;  
451 Kellogg et al., 2020; Morel et al., 2020; Price and Morel, 1990; Sunda and Huntsman, 1995;  
452 Timmermans et al., 2001; Xu et al., 2007; Yee and Morel, 1996). However, in certain organisms such  
453 as in the coccolithophore *Emiliana huxleyi*, it is possible that Co is the preferred metal co-factor since  
454 the growth rate was higher under replete Co than under replete Zn. One reason could be the  
455 simultaneous development of ocean chemistry and cyanobacterial metabolism under the Co- and Fe-  
456 replete, but Zn-deplete conditions of the ancient ocean ~2.5 Gyr ago (Dupont et al., 2006; Johnson et  
457 al., 2024; Saito et al., 2003). Another explanation for Co use in alkaline phosphatases may require  
458 maintaining low intracellular availability of Zn to avoid toxicity through inhibition of Co insertion by  
459 high Zn into cobalamin (Hawco and Saito, 2018). Supporting this, the cyanobacterium *Synechococcus*  
460 *bacillaris* and *Prochlorococcus* were found to have absolute Co requirements for growth (Sunda and  
461 Huntsman, 1995). Together with these aspects, our insights from the bioassay response at 54 °W  
462 merits further investigations into whether *Synechococcus* can interchange Zn and Co in PhoA, and  
463 indeed which metal is preferred. This would be an important insight for considerations of  
464 stoichiometric plasticity and niche partitioning across the vast Zn- and Co-depleted regions of the  
465 ocean, especially where dZn can become depleted to levels similar or below dCo (Kellogg et al.,  
466 2020).

467 Across all bioassays, the addition of Zn did not increase the concentration of any presumably  
468 Fe-dependent PhoX, and the addition of Fe did not increase the concentration of any presumably Zn-  
469 or Co-dependent PhoA. In other words, no significant unexpected responses were observed.  
470 Nevertheless, there are some non-significant trends upon the addition of Co that warrant further study.  
471 For example, the addition of Co increased the putative Fe-containing *Prochlorococcus* PhoX protein  
472 concentration dramatically in one of the replicates at 45 °W and hence, Co could be an efficient metal  
473 co-factor in PhoX (as in the bacterium *Pasteurella multocida* (Wu, Jin-Ru et al., 2007)), or at least,  
474 directly or indirectly stimulate production of PhoX. This contrasts with the results of Kathuria &  
475 Martiny (Kathuria and Martiny, 2011), who hypothesized an enzyme inhibiting role of Co (and Zn;  
476 with Fe untested) for the activity of both *Synechococcus* and *Prochlorococcus* PhoX by replacing  
477  $\text{Ca}^{2+}$  at the active site.

478 Taken together, the results of our bioassays suggest that alkaline phosphatase enzymes are  
479 affected by trace metal concentrations, and that the response to Zn, Co or Fe may be species or strain  
480 specific. The metal effects differed between the responsive enzyme type (PhoA versus PhoX) and  
481 phytoplankton species (*Prochlorococcus* versus *Synechococcus*) at contrasting biogeochemical  
482 settings across the basin. It is plausible that the significant changes in protein concentration can result  
483 directly from the metal addition triggering more alkaline phosphatase production per cell. This  
484 demonstrates that the cycling of macronutrients and metals are intermittently linked and that the  
485 nature of that linkage depends on microbial community composition

**Deleted:** co-evolution of

**Deleted:** cobalt

488 **Towards a quantitative, *in situ* marine metalloproteome of *Synechococcus***

489 An advantage of absolute quantitative measurements over relative proteomics data is the ability to  
 490 relate the absolute protein concentrations to other data types, including biological rate measurements  
 491 and cellular metal stoichiometry. To this end, the concentrations of the Zn, Co or Fe-dependent  
 492 alkaline phosphatases measured in this study naturally lead to two questions: First, how much metal is  
 493 allocated as alkaline phosphatase co-factors in the cell, and how does this compare to total cellular  
 494 metal content? Second, how does the APA estimated from enzyme abundance compare to assay-based  
 495 APA?

496 To address these questions, model calculations were performed. Variables other than the  
 497 absolute concentrations of the alkaline phosphatases were either measured concomitantly during the  
 498 bioassays, such as cellular metal quotas, cell abundance, APA and DOP concentration, or sourced  
 499 from the literature such as strain specific contribution to cell abundance, phosphoester contribution to  
 500 the DOP pool, enzyme kinetics parameters and subcellular enzyme localization (Table S7). We chose  
 501 to use the *Synechococcus* PhoA concentrations in the control treatments at 54 °W after 48 h in these  
 502 calculations for three reasons: First, cellular metal quotas of *Synechococcus* but not of  
 503 *Prochlorococcus* were measured in this treatment, due to limited sampling capacity and small cell  
 504 sizes for *Prochlorococcus* (Sofen et al., 2022). Second, enzyme kinetics parameters of the PhoA  
 505 rather than the PhoX isoform are well documented in the literature (Lazdunski and Lazdunski, 1969).  
 506 Third, estimates for the contribution of *Synechococcus* strain WH8102 (to which our measured PhoA  
 507 is specific) to total *Synechococcus* counts exist from previous studies nearest to 54 °W (Ohnemus et  
 508 al., 2016). A similar reasoning applied to the phosphoester contribution to the DOP pool. For ease,  
 509 more detailed explanations, all values, and assumptions are in Tables S3 and S4.

510 Equation 1a approximates the cellular Zn allocation towards the *Synechococcus* PhoA from  
 511 the replicate-averaged PhoA concentration in seawater normalised to cell abundance, assuming full  
 512 metalation of the enzyme with four metal ions per dimer (Coleman, 1992). The cell abundance is a  
 513 function of *Synechococcus* cell counts and the fractional abundance of strain WH8102, to which the  
 514 measured PhoA is specific. Equation 1b expresses the results of Equation 1a as a fraction of the total  
 515 cellular Zn content.

516 Allocated  $Zn_{PhoA} = \text{metalated co-factors}_{PhoA} \times PhoA_{sw} / (\text{Syn. abundance} \times \text{WH8102 fraction})$  (1a)

517 Fractional allocated  $Zn_{PhoA} = Zn_{PhoA} / Zn_{\text{total cell}}$  (1b)

518 The amount of metal allocated to PhoA in *Synechococcus* is 3,054 atoms cell<sup>-1</sup>. This translates  
 519 to a maximum fractional contribution towards the total cellular Zn content of 0.66 % after dividing by  
 520 cellular Zn measured using SXRF (Table S1). If the co-factor in PhoA is assumed to be occupied by

**Deleted: Alkaline phosphatase abundances in the context of bulk community APA**

Alkaline phosphatase activity and phytoplankton biomass (by Chl-a proxy) did not increase significantly upon the metal additions in the bioassays, neither together with the responses observed in the absolute enzyme concentrations at 54 °W, 45 °W and 31 °W, nor in any other treatments or locations (also Mahaffey et al.; submitted). A quantitative explanation for this – and hence a demonstration of the power of proteomics on the organism level – emerges from estimates of enzyme abundance-based enzyme rates, where the APA assay covers the entire microbial community (i.e. everything from bacteria to eukaryotes) but the proteomics measurements are specific to a subset of *Prochlorococcus* and *Synechococcus*. 

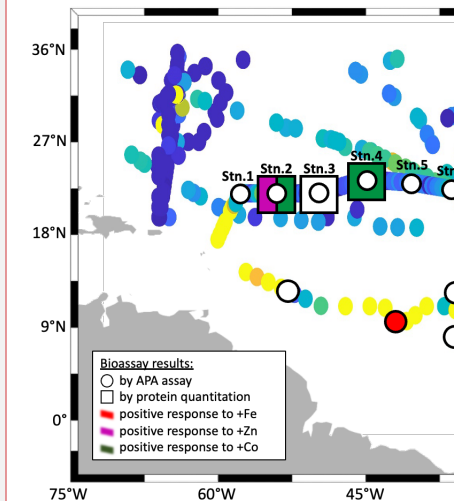


Figure 3 Map of the North Atlantic showing surface phosphate concentrations (compiled by Martiny et al., 2019 (Martiny et al., 2019); augmented with data from Browning et al. 2017 (Browning et al., 2017)). Overlain are locations of bioassays, where the response of APA to metal additions was tested (circles), and of bioassays, where the absolute concentration of the alkaline phosphatase proteins was measured in response to metal additions (squares). Bioassays of the present study include longitudinal station labels. The others are from Mahaffey et al. (2014) (Mahaffey et al., 2014) and Browning et al. (2017) (Browning et al., 2017) as well as from additional bioassays during JC150 (Mahaffey et al. (submitted as a companion to this article), but where no protein measurements were made. Symbols at bioassay locations are coloured in red, purple or green, if a positive response was observed upon addition of Fe, Zn or Co respectively. 

**Formatted:** Font: Italic

**Formatted:** Font: Italic

**Deleted:** 1

**Deleted:** 2

**Deleted:** \*

**Deleted:** \*

613 Co<sup>2+</sup> instead of Zn<sup>2+</sup>, the fractional contribution to the cellular Co content is 38 %, due to the lower  
 614 total cellular Co content of *Synechococcus* compared to Zn (Table S1). It is possible that the active  
 615 sites of PhoA are occupied by a mixture of Zn and Co, incompletely metalated, or under competition  
 616 by metals other than Zn or Co. Nevertheless, these low fractional contributions of PhoA-allocated Zn  
 617 appear biochemically reasonable, as the majority of Zn in *Synechococcus* appears to be stored in  
 618 metallothioneins to maintain Zn homeostasis and potentially supply alkaline phosphatases with Zn as  
 619 needed (Cox and Saito, 2013; Mikhaylina et al., 2022). However, our bioassay results also suggest Zn  
 620 may not be the preferred co-factor in *Synechococcus* PhoA: The larger response of this enzyme to Co  
 621 additions at 54 °W suggests the effective substitution of or even preference for Co (Fig. 2). This  
 622 aligns with evolutionary arguments (see 'Metal control on alkaline phosphatases') and imply that  
 623 PhoA is a potential major sink of cellular Co. This also implies that *Synechococcus* growth may be  
 624 sensitive towards Co-phosphorus co-limitation in the oligotrophic ocean.

**Deleted:** would align  
**Deleted:** would  
**Deleted:** y

625 Equation 2a approximates the *Synechococcus* PhoA-abundance based hydrolysis rate as a  
 626 function of the PhoA concentration (converting molarity units to grams using its molecular weight),  
 627 phosphoester substrate concentration, and Michaelis-Menten kinetics parameters V<sub>max</sub> and K<sub>m</sub>, the  
 628 maximum reaction rate and half-saturation constant, respectively, derived from an *E. coli* homologue  
 629 of PhoA (Table S2). Equation 2b expresses the results of Equation 2a as a fraction of the 'total APA',  
 630 a function of the measured MUF-P assay-based APA with a correction applied for the subcellular  
 631 localisation of marine alkaline phosphatases, of which only the periplasmic-outwards fraction (~20 to  
 632 80 %) is detectable via the MUF-P assay. In other words, the calculated 'total APA' accounts for both  
 633 the dissolved and particulate activity. Details on made assumptions are in the supplement (Table S2).

634 Rate<sub>PhoA</sub> = PhoA<sub>SW</sub> ~~×~~ molecular weight ~~×~~ V<sub>max</sub> ~~×~~ substrate / (substrate + K<sub>m</sub>) (2a)  
 635 where substrate = DOP ~~×~~ phosphoester fraction  
 636 Fractional Rate<sub>PhoA</sub> = Rate<sub>PhoA</sub> ~~×~~ periplasmic-outwards fraction / assayed APA (2b)

**Deleted:** \*  
**Deleted:** \*  
**Deleted:** \*  
**Deleted:** \*  
**Deleted:** \*

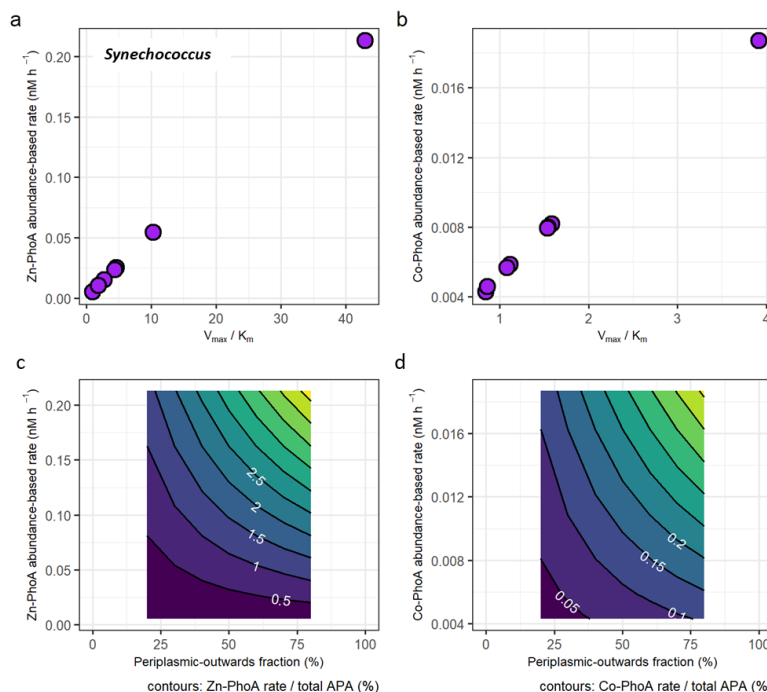
637 The protein abundance-based rates range from 0.00517 nM h<sup>-1</sup> to 0.213 nM h<sup>-1</sup> for the Zn-  
 638 dependent *Synechococcus* PhoA and from 0.00428 nM h<sup>-1</sup> to 0.0187 nM h<sup>-1</sup> for the Co-dependent  
 639 PhoA (Fig. 4a and b), using the *E. coli* kinetics parameters for each metal that are slower under Co  
 640 coordination. In terms of fractional contributions to total APA, the rate estimates translate to  
 641 maximally 5.2 % for Zn-PhoA and 0.46 % for the Co-PhoA. Regardless of the choice of enzyme  
 642 kinetics, it appeared that *Synechococcus* PhoA contributed a small component to the total APA in our  
 643 bioassays. This concurs with the observed increase in concentration of *Synechococcus* PhoA upon  
 644 metal addition versus the null response in APA. Applying the same calculation and kinetics  
 645 parameters for the case of the *Prochlorococcus* PhoA yields abundance-based rates between 0.03 ~~5~~ Deleted: 47

655 nM h<sup>-1</sup> and 1.4 nM h<sup>-1</sup> for the Zn-PhoA and between 0.029 nM h<sup>-1</sup> and 0.13 nM h<sup>-1</sup> for the Co-PhoA,  
 656 which translate to maximal contributions to the total APA of 35 % and 3.1 %, respectively. These  
 657 higher rates and fractional contributions compared to the *Synechococcus* PhoA are due to the higher  
 658 concentrations of the *Prochlorococcus* PhoA than the *Synechococcus* PhoA in the chosen samples.  
 659 The taxon-specific alkaline phosphatase concentrations illustrate the challenge of interpreting bulk  
 660 enzyme activities when the functional enzyme class is produced by many biological taxa  
 661 (cyanobacteria, heterotrophic bacteria, diatoms etc.). In essence, the different bioassay responses  
 662 shown here demonstrate the need to further develop a “meta-biochemistry” capability to understand  
 663 biogeochemical reactions at the mechanistic level.

**Deleted:** 2

**Deleted:** 87

**Deleted:** 25



680 periplasmic location of alkaline phosphatase has been observed to result in loss during preservation.  
681 In a preservation study, PhoA was notably the protein with the lowest recovery in *Synechococcus*  
682 WH8102 after a month in storage compared to  $101\% \pm 27\%$  for the fifty most abundant proteins(Saito  
683 et al., 2011a). The combination of multiple abundant and rare microbial sources of alkaline  
684 phosphatases together contribute to the particulate, and when secreted or lost, dissolved reservoirs that  
685 make up the bulk APA.

## 686 **Conclusions**

687 This study performs taxon-specific alkaline phosphatase isoform analysis via absolute quantitative  
688 proteomics on *Prochlorococcus* and *Synechococcus*, coupled to enzyme bioassays. This approach  
689 supports the use of Zn, Co and Fe in alkaline phosphatases in the natural oceanic environment, but  
690 also adds complexity to our understanding of how these enzymes are regulated in a biogeochemical  
691 context. Our mechanistic perspective revealed that these two highly abundant microbes are only  
692 minor contributors to bulk APA, which carries important implications for the interpretation of the  
693 widely used fluorescent APA assay. Additionally, within this picocyanobacterial class, we observed  
694 heterogeneous responses of the alkaline phosphatase enzymes depending on the protein, taxonomy,  
695 biogeochemical context, and treatment. This indicates that there is significant biological diversity in  
696 the responses of individual marine organisms to experimental treatments that can be resolved by  
697 combining enzyme assay measurements with quantitative proteomics. Our results indicate a need for  
698 biochemical characterisation of key marine alkaline phosphatases, particularly with regards to their  
699 kinetics and metal co-factors as highlighted by the potential importance of Co as a metal co-factor in  
700 PhoA and possibly PhoX. Future efforts to understand the biochemical properties of marine microbes  
701 will benefit the connected interpretation of molecular, enzymatic, and biogeochemical assays, and in  
702 turn our understanding of nutrient cycling in the ocean system.

## 703 **Acknowledgements**

704 The authors would like to thank the captain and crew of the *R.R.S. James Cook* during cruise JC150,  
705 as well as all the scientific party members, who helped to conduct the bioassays. The authors would  
706 also like to thank Alastair Lough and Clément Demasy for the dCo measurements, and Julie Robidart  
707 and Rosalind Rickaby for fruitful discussions on this manuscript. This research was supported by the  
708 National Environmental Research Council (UK) under grants NE/N001125/1 to MCL and  
709 NE/N001079/1 to CM, by the National Science Foundation (USA) under grant OCE1829819 to BST,  
710 OCE1924554, OCE1850719 and NIH R01GM135709 to MAS, and by the Graduate School of the  
711 National Oceanography Centre Southampton (UK) to KK. The writing process was also supported by  
712 the Simons Foundation under award 723552 to KK and by the the USC Dornsife College of Arts and  
713 Sciences to NAH. [\[This research used resources of the Advanced Photon Source, a U.S. Department](#)

**Formatted:** Font: (Default) Times New Roman

714 of Energy (DOE) Office of Science user facility operated for the DOE Office of Science by Argonne  
715 National Laboratory under Contract No. DE-AC02-06CH11357.

716 **Author contributions:** NAH and KK wrote the initial manuscript draft. NAH and KK performed the  
717 proteomics analysis with help from MM and MAS. KK, NAH, NJW, CD, CM, MCL performed the  
718 experiments at sea. BST and ELM conducted the cell quota measurements. MCL, CM, AT and MAS  
719 led the research campaign. All authors commented on the manuscript.

720 **Competing interests:** The authors declare no competing interests.

721 **Data Availability:** Source data for all main and supplementary figures are provided in the  
722 supplement. The mass spectrometry proteomics data have been deposited to the ProteomeXchange  
723 Consortium via the PRIDE [1] partner repository with the dataset identifier PXD053717.

**Commented [BT3]:** Please add this acknowledgement required for all samples run at US synchrotron.

**Formatted:** Font: (Default) Times New Roman, 11 pt

724 **References**

- 725 Bicknell, R., Schaeffer, A., Auld, D. S., Riordan, J. F., Monnanni, R., and Bertini, I.: Protease  
726 susceptibility of zinc - and APO-carboxypeptidase A, *Biochemical and Biophysical Research*  
727 *Communications*, 133, 787–793, [https://doi.org/10.1016/0006-291X\(85\)90973-8](https://doi.org/10.1016/0006-291X(85)90973-8), 1985.
- 728 Bradshaw, R. A., Cancedda, F., Ericsson, L. H., Neumann, P. A., Piccoli, S. P., Schlesinger, M. J.,  
729 Shriefer, K., and Walsh, K. A.: Amino acid sequence of *Escherichia coli* alkaline phosphatase., *Proc.*  
730 *Natl. Acad. Sci. U.S.A.*, 78, 3473–3477, <https://doi.org/10.1073/pnas.78.6.3473>, 1981.
- 731 Browning, T. J., Achterberg, E. P., Yong, J. C., Rapp, I., Utermann, C., Engel, A., and Moore, C. M.: Iron  
732 limitation of microbial phosphorus acquisition in the tropical North Atlantic, *Nature*  
733 *Communications*, 8, 1–7, <https://doi.org/10.1038/ncomms15465>, 2017.
- 734 Carvalho, P. C., Fischer, J. S. G., Chen, E. I., Yates, J. R., and Barbosa, V. C.: PatternLab for proteomics:  
735 A tool for differential shotgun proteomics, *BMC Bioinformatics*, 9, 1–14,  
736 <https://doi.org/10.1186/1471-2105-9-316>, 2008.
- 737 Coleman, J. E.: Structure and mechanism of alkaline phosphatase, *Annu Rev Biophys Biomol Struct*,  
738 21, 441–483, <https://doi.org/10.1146/annurev.bb.21.060192.002301>, 1992.
- 739 Cox, A. D. and Saito, M. A.: Proteomic responses of oceanic *Synechococcus* WH8102 to phosphate  
740 and zinc scarcity and cadmium additions, *Frontiers in Microbiology*, 4, 1–17,  
741 <https://doi.org/10.3389/fmicb.2013.00387>, 2013.
- 742 Davis, C., Lohan, M. C., Tuerena, R., Cerdan-Garcia, E., Woodward, E. M. S., Tagliabue, A., and  
743 Mahaffey, C.: Diurnal variability in alkaline phosphatase activity and the potential role of  
744 zooplankton, *Limnology and Oceanography Letters*, 4, 71–78, <https://doi.org/10.1002/lo2.10104>,  
745 2019.
- 746 Duhamel, S., Dyrhman, S. T., and Karl, D. M.: Alkaline phosphatase activity and regulation in the  
747 North Pacific Subtropical Gyre, *Limnology and Oceanography*, 55, 1414–1425,  
748 <https://doi.org/10.4319/lo.2010.55.3.1414>, 2010.
- 749 Duhamel, S., Bjo, K. M., Wambeke, F. V., Moutin, T., and Karl, D. M.: Characterization of alkaline  
750 phosphatase activity in the North and South Pacific Subtropical Gyres : Implications for phosphorus  
751 cycling, 56, 1244–1254, <https://doi.org/10.4319/lo.2011.56.4.1244>, 2011.
- 752 Dupont, C. L., Yang, S., Palenik, B., and Bourne, P. E.: Modern proteomes contain putative imprints of  
753 ancient shifts in trace metal geochemistry., *Proceedings of the National Academy of Sciences of the*  
754 *United States of America*, 103, 17822–7, <https://doi.org/10.1073/pnas.0605798103>, 2006.
- 755 Dyrhman, S. T. and Ruttenberg, K. C.: Presence and regulation of alkaline phosphatase activity in  
756 eukaryotic phytoplankton from the coastal ocean: Implications for dissolved organic phosphorus  
757 remineralization, *Limnology and Oceanography*, 51, 1381–1390,  
758 <https://doi.org/10.4319/lo.2006.51.3.1381>, 2006.
- 759 Gottesman, M., Simpson, R. T., and Vallee, B. L.: Kinetic properties of cobalt alkaline phosphatase,  
760 *Biochemistry*, 8, 3776–3783, <https://doi.org/10.1021/bi00837a043>, 1969.
- 761 Hawco, N. J. and Saito, M. A.: Competitive inhibition of cobalt uptake by zinc and manganese in a  
762 pacific *Prochlorococcus* strain: Insights into metal homeostasis in a streamlined oligotrophic

- 763 cyanobacterium, Limnology and Oceanography, 63, 2229–2249, <https://doi.org/10.1002/lno.10935>,  
764 2018.
- 765 Held, N. A., Webb, E. A., McIlvin, M. M., Hutchins, D. A., Cohen, N. R., Moran, D. M., Kunde, K.,  
766 Lohan, M. C., Mahaffey, C. M., Woodward, E. M. S., and Saito, M. A.: Co-occurrence of Fe and P  
767 stress in natural populations of the marine diazotroph *Trichodesmium*, Biogeosciences, 17, 2537–  
768 2551, <https://doi.org/10.5194/bg-2019-493>, 2020.
- 769 Hoffmann, L. J., Breitbarth, E., Boyd, P. W., and Hunter, K. A.: Influence of ocean warming and  
770 acidification on trace metal biogeochemistry, Marine Ecology Progress Series, 470, 191–205,  
771 <https://doi.org/10.3354/meps10082>, 2012.
- 772 Jakuba, R. Wisniewski, Moffett, J. W., and Dyhrman, S. T.: Evidence for the linked biogeochemical  
773 cycling of zinc, cobalt, and phosphorus in the western North Atlantic Ocean, Global Biogeochemical  
774 Cycles, 22, 2008.
- 775 Johnson, J. E., Present, T. M., and Valentine, J. S.: Iron: Life's primeval transition metal, Proceedings  
776 of the National Academy of Sciences, 121, e2318692121, <https://doi.org/10.1073/pnas.2318692121>,  
777 2024.
- 778 Kathuria, S. and Martiny, A. C.: Prevalence of a calcium-based alkaline phosphatase associated with  
779 the marine cyanobacterium *Prochlorococcus* and other ocean bacteria, Environ Microbiol, 13, 74–  
780 83, <https://doi.org/10.1111/j.1462-2920.2010.02310.x>, 2011.
- 781 Kellogg, R. M., McIlvin, M. R., Vedamati, J., Twining, B. S., Moffett, J. W., Marchetti, A., Moran, D. M.,  
782 and Saito, M. A.: Efficient zinc/cobalt inter-replacement in northeast Pacific diatoms and relationship  
783 to high surface dissolved Co : Zn ratios, Limnology and Oceanography, 65, 2557–2582,  
784 <https://doi.org/10.1002/lno.11471>, 2020.
- 785 Kim, I.-N., Lee, K., Gruber, N., Karl, D. M., Bullister, J. L., Yang, S., and Kim, T.-W.: Chemical  
786 oceanography. Increasing anthropogenic nitrogen in the North Pacific Ocean, Science, 346, 1102–  
787 1106, <https://doi.org/10.1126/science.1258396>, 2014.
- 788 Kolowith, L. C., Ingall, E. D., and Benner, R.: Composition and cycling of marine organic phosphorus,  
789 Limnology & Oceanography, 46, 309–320, <https://doi.org/10.4319/lo.2001.46.2.0309>, 2001.
- 790 Kunde, K., Wyatt, N. J., González-Santana, D., Tagliabue, A., Mahaffey, C., and Lohan, M. C.: Iron  
791 Distribution in the Subtropical North Atlantic: The Pivotal Role of Colloidal Iron, Global  
792 Biogeochemical Cycles, 2019GB006326, <https://doi.org/10.1029/2019GB006326>, 2019.
- 793 Lazdunski, C. and Lazdunski, M.: Zn<sup>2+</sup> and Co<sup>2+</sup>-alkaline phosphatases of *E. coli*. A comparative  
794 kinetic study, Eur J Biochem, 7, 294–300, <https://doi.org/10.1111/j.1432-1033.1969.tb19606.x>,  
795 1969.
- 796 Li, H., Veldhuis, M., and Post, A.: Alkaline phosphatase activities among planktonic communities in  
797 the northern Red Sea, Mar. Ecol. Prog. Ser., 173, 107–115, <https://doi.org/10.3354/meps173107>,  
798 1998.
- 799 Lohan, M. C. and Tagliabue, A.: Oceanic Micronutrients: Trace Metals that are Essential for Marine  
800 Life, Elements, 14, 385–390, <https://doi.org/10.2138/gselements.14.6.385>, 2018.

- 801 Lomas, M. W., Burke, A. L., Lomas, D. A., Bell, D. W., Shen, C., Dyhrman, S. T., and Ammerman, J. W.:  
802 Sargasso Sea phosphorus biogeochemistry: an important role for dissolved organic phosphorus  
803 (DOP), *Biogeosciences*, 7, 695–710, <https://doi.org/10.5194/bg-7-695-2010>, 2010.
- 804 Lu, X. and Zhu, H.: Tube-Gel Digestion: A Novel Proteomic Approach for High Throughput Analysis of  
805 Membrane Proteins, *Mol Cell Proteomics*, 4, 1948–1958, <https://doi.org/10.1074/mcp.M500138-MCP200>, 2005.
- 807 Lundgren, D. H., Hwang, S. I., Wu, L., and Han, D. K.: Role of spectral counting in quantitative  
808 proteomics, *Expert Review of Proteomics*, 7, 39–53, <https://doi.org/10.1586/epr.09.69>, 2010.
- 809 Luo, H., Benner, R., Long, R. A., and Hu, J.: Subcellular localization of marine bacterial alkaline  
810 phosphatases, *Proceedings of the National Academy of Sciences of the United States of America*,  
811 106, 21219–21223, <https://doi.org/10.1073/pnas.0907586106>, 2009.
- 812 MacLean, B., Tomazela, D. M., Shulman, N., Chambers, M., Finney, G. L., Frewen, B., Kern, R., Tabb,  
813 D. L., Liebler, D. C., and MacCoss, M. J.: Skyline: an open source document editor for creating and  
814 analyzing targeted proteomics experiments, *Bioinformatics*, 26, 966–968,  
815 <https://doi.org/10.1093/bioinformatics/btq054>, 2010.
- 816 Mahaffey, C., Reynolds, S., Davis, C. E., Lohan, M. C., and Lomas, M. W.: Alkaline phosphatase  
817 activity in the subtropical ocean: insights from nutrient, dust and trace metal addition experiments,  
818 *Frontiers in Marine Science*, 1, 1–13, <https://doi.org/10.3389/fmars.2014.00073>, 2014.
- 819 Martiny, A. C., Coleman, M. L., and Chisholm, S. W.: Phosphate acquisition genes in *Prochlorococcus*  
820 ecotypes: Evidence for genome-wide adaptation, *Proceedings of the National Academy of Sciences*,  
821 103, 12552–12557, <https://doi.org/10.1073/pnas.0601301103>, 2006.
- 822 Martiny, A. C., Lomas, M. W., Fu, W., Boyd, P. W., Chen, Y. L., Cutter, G. A., Ellwood, M. J., Furuya, K.,  
823 Hashihama, F., Kanda, J., Karl, D. M., Kodama, T., Li, Q. P., Ma, J., Moutin, T., Woodward, E. M. S.,  
824 and Moore, J. K.: Biogeochemical controls of surface ocean phosphate, *Science Advances*, 5,  
825 eaax0341, <https://doi.org/10.1126/sciadv.aax0341>, 2019.
- 826 Mather, R., Reynolds, S., Wolff, G., Williams, R., Torres-Valdés, S., Woodward, E., Angela, L., Pan, X.,  
827 Sanders, R., and Achterberg, E.: Phosphorus cycling in the North and South Atlantic Ocean  
828 subtropical gyres, *Nature Geoscience*, 1, 439–443, <https://doi.org/10.1038/ngeo232>, 2008.
- 829 Mikhaylina, A., Scott, L., Scanlan, D. J., and Blindauer, C. A.: A metallothionein from an open ocean  
830 cyanobacterium removes zinc from the sensor protein controlling its transcription, *J Inorg Biochem*,  
831 230, 111755, <https://doi.org/10.1016/j.jinorgbio.2022.111755>, 2022.
- 832 Moore, C. M., Mills, M. M., Arrigo, K. R., Berman-Frank, I., Bopp, L., Boyd, P. W., Galbraith, E. D.,  
833 Geider, R. J., Guieu, C., Jaccard, S. L., Jickells, T. D., Roche, J. L., Lenton, T. M., Mahowald, N. M.,  
834 Marañón, E., Marinov, I., Moore, J. K., Nakatsuka, T., Oschlies, A., Saito, M. A., Thingstad, T. F.,  
835 Tsuda, A., and Ulloa, O.: Processes and Patterns of Oceanic Nutrient Limitation, *Nat Geoscience*, 6,  
836 701–710, 2013.
- 837 Morel, F. M. M., Lam, P. J., and Saito, M. A.: Trace Metal Substitution in Marine Phytoplankton,  
838 Annual Review of Earth and Planetary Sciences, 48, 491–517, <https://doi.org/10.1146/annurev-earth-053018-060108>, 2020.

- 840 Ohnemus, D. C., Rauschenberg, S., Krause, J. W., Brzezinski, M. A., Collier, J. L., Geraci-Yee, S., Baines,  
841 S. B., and Twining, B. S.: Silicon content of individual cells of *Synechococcus* from the North Atlantic  
842 Ocean, *Marine Chemistry*, 187, 16–24, <https://doi.org/10.1016/j.marchem.2016.10.003>, 2016.
- 843 Price, N. M. and Morel, F. M. M.: Cadmium and cobalt substitution for zinc in a marine diatom,  
844 *Nature*, 344, 658–660, <https://doi.org/10.1038/344658a0>, 1990.
- 845 Saito, M., Alexander, H., Benway, H., Boyd, P., Gledhill, M., Kujawinski, E., Levine, N., Maheigan, M.,  
846 Marchetti, A., Obernosterer, I., Santoro, A., Shi, D., Suzuki, K., Tagliabue, A., Twining, B., and  
847 Maldonado, M.: The Dawn of the BioGeoSCAPES Program: Ocean Metabolism and Nutrient Cycles  
848 on a Changing Planet, *Oceanog*, 37, <https://doi.org/10.5670/oceanog.2024.417>, 2024.
- 849 Saito, M. A., Sigman, D. M., and Morel, F. M. M.: The bioinorganic chemistry of the ancient ocean:  
850 The co-evolution of cyanobacterial metal requirements and biogeochemical cycles at the Archean-  
851 Proterozoic boundary?, *Inorganica Chimica Acta*, 356, 308–318, [https://doi.org/10.1016/S0020-1693\(03\)00442-0](https://doi.org/10.1016/S0020-1693(03)00442-0), 2003.
- 853 Saito, M. A., Bulygin, V. V., Moran, D. M., Taylor, C., and Scholin, C.: Examination of Microbial  
854 Proteome Preservation Techniques Applicable to Autonomous Environmental Sample Collection,  
855 *Front Microbiol*, 2, 215, <https://doi.org/10.3389/fmicb.2011.00215>, 2011a.
- 856 Saito, M. A., Bertrand, E. M., Dutkiewicz, S., Bulygin, V. V., Moran, D. M., Monteiro, F. M., Follows,  
857 M. J., Valois, F. W., and Waterbury, J. B.: Iron conservation by reduction of metalloenzyme  
858 inventories in the marine diazotroph *Crocospaera watsonii*., *Proceedings of the National Academy  
859 of Sciences of the United States of America*, 108, 2184–9,  
860 <https://doi.org/10.1073/pnas.1006943108>, 2011b.
- 861 Saito, M. A., McIlvin, M. R., Moran, D. M., Goepfert, T. J., DiTullio, G. R., Post, A. F., and Lamborg, C.  
862 H.: Multiple nutrient stresses at intersecting Pacific Ocean biomes detected by protein biomarkers.,  
863 *Science* (New York, N.Y.), 345, 1173–7, <https://doi.org/10.1126/science.1256450>, 2014.
- 864 Saito, M. a., Dorsk, A., Post, A. F., McIlvin, M. R., Rappé, M. S., DiTullio, G. R., and Moran, D. M.:  
865 Needles in the blue sea: Sub-species specificity in targeted protein biomarker analyses within the  
866 vast oceanic microbial metaproteome, *Proteomics*, <https://doi.org/10.1002/pmic.201400630>, 2015.
- 867 Saito, M. A., Noble, A. E., Hawco, N., Twining, B. S., Ohnemus, D. C., John, S. G., Lam, P., Conway, T.  
868 M., Johnson, R., Moran, D., and McIlvin, M.: The acceleration of dissolved cobalt's ecological  
869 stoichiometry due to biological uptake, remineralization, and scavenging in the Atlantic Ocean,  
870 *Biogeosciences*, 14, 4637–4662, <https://doi.org/10.5194/bg-14-4637-2017>, 2017.
- 871 Saito, M. A., McIlvin, M. R., Moran, D. M., Santoro, A. E., Dupont, C. L., Rafter, P. A., Saunders, J. K.,  
872 Kaul, D., Lamborg, C. H., Westley, M., Valois, F., and Waterbury, J. B.: Abundant nitrite-oxidizing  
873 metalloenzymes in the mesopelagic zone of the tropical Pacific Ocean, *Nature Geoscience*, 13,  
874 <https://doi.org/10.1038/s41561-020-0565-6>, 2020.
- 875 Santos-Benito, F.: The Pho regulon: a huge regulatory network in bacteria, *Frontiers in Microbiology*,  
876 6, 1–14, <https://doi.org/10.3389/fmicb.2015.00402>, 2015.
- 877 Saunders, J. K., Gaylord, D. A., Held, N. A., Symmonds, N., Dupont, C., Shepherd, A., Kinkade, D. B.,  
878 and Saito, M. A.: METATRYP v 2.0: Metaproteomic Least Common Ancestor Analysis for Taxonomic  
879 Inference Using Specialized Sequence Assemblies - Standalone Software and Web Servers for Marine  
880 Microorganisms and Coronaviruses, *Journal of Proteome Research*,  
881 <https://doi.org/10.1021/acs.jproteome.0c00385>, 2020.

- 882 Scanlan, D. J., Mann, N. H., and Carr, N. G.: The response of the picoplanktonic marine  
883 cyanobacterium *Synechococcus* species WH7803 to phosphate starvation involves a protein  
884 homologous to the periplasmic phosphate-binding protein of *Escherichia coli*, *Mol Microbiol*, 10,  
885 181–191, <https://doi.org/10.1111/j.1365-2958.1993.tb00914.x>, 1993.
- 886 Shaked, Y., Xu, Y., Leblanc, K., and Morel, F. M. M.: Zinc availability and alkaline phosphatase activity  
887 in *Emiliania huxleyi*: Implications for Zn-P co-limitation in the ocean, *Limnology and Oceanography*,  
888 51, 299–309, <https://doi.org/10.4319/lo.2006.51.1.0299>, 2006.
- 889 Sofen, L. E., Antipova, O. A., Ellwood, M. J., Gilbert, N. E., LeCleir, G. R., Lohan, M. C., Mahaffey, C.,  
890 Mann, E. L., Ohnemus, D. C., Wilhelm, S. W., and Twining, B. S.: Trace metal contents of autotrophic  
891 flagellates from contrasting open-ocean ecosystems, *Limnology and Oceanography Letters*, 7, 354–  
892 362, <https://doi.org/10.1002/lol2.10258>, 2022.
- 893 Sunda, W. G. and Huntsman, S. A.: Cobalt and zinc interreplacement in marine phytoplankton:  
894 Biological and geochemical implications, *Limnology and Oceanography*, 40, 1404–1417,  
895 <https://doi.org/10.4319/lo.1995.40.8.1404>, 1995.
- 896 Timmermans, K. R., Snoek, J., Gerringa, L. J. A., Zondervan, I., and de Baar, H. J. W.: Not all eukaryotic  
897 algae can replace zinc with cobalt: *Chaetoceros calcitrans* (Bacillariophyceae) versus *Emiliania*  
898 *huxleyi* (Prymnesiophyceae), *Limnology and Oceanography*, 46, 699–703,  
899 <https://doi.org/10.4319/lo.2001.46.3.0699>, 2001.
- 900 Wiśniewski, J. R. and Rakus, D.: Quantitative analysis of the *Escherichia coli* proteome, *Data Brief*, 1,  
901 7–11, <https://doi.org/10.1016/j.dib.2014.08.004>, 2014.
- 902 Wojciechowski, C. L., Cardia, J. P., and Kantrowitz, E. R.: Alkaline phosphatase from the  
903 hyperthermophilic bacterium *T. maritima* requires cobalt for activity - Wojciechowski - 2002 -  
904 Protein Science - Wiley Online Library, *Protein Science*, 11, 903–911, n.d.
- 905 Wu, Jin-Ru, Shien, Jui-Hung, Shieh, Happy K., Hu, Chung-Chi, Gong, Shuen-Rong, Chen, Ling-Yun, and  
906 Chang, Poa-Chun: Cloning of the gene and characterization of the enzymatic properties of the  
907 monomeric alkaline phosphatase (PhoX) from *Pasteurella multocida* strain X-73, *FEMS Microbiology*  
908 Letters
- 909 Wurl, O., Zimmer, L., and Cutter, G. A.: Arsenic and phosphorus biogeochemistry in the ocean:  
910 Arsenic species as proxies for P-limitation, *Limnology and Oceanography*, 58, 729–740,  
911 <https://doi.org/10.4319/lo.2013.58.2.0729>, 2013.
- 912 Xu, Y., Tang, D., Shaked, Y., and Morel, F. M. M.: Zinc, cadmium, and cobalt interreplacement and  
913 relative use efficiencies in the coccolithophore *Emiliania huxleyi*, *Limnology and Oceanography*, 52,  
914 2294–2305, <https://doi.org/10.4319/lo.2007.52.5.2294>, 2007.
- 915 Yee, D. and Morel, F. M. M.: In vivo substitution of zinc by cobalt in carbonic anhydrase of a marine  
916 diatom, *Limnology and Oceanography*, 41, 573–577, <https://doi.org/10.4319/lo.1996.41.3.0573>,  
917 1996.
- 918 Yong, S. C., Roversi, P., Lillington, J., Rodriguez, F., Krehenbrink, M., Zeldin, O. B., Garman, E. F., Lea,  
919 S. M., and Berks, B. C.: A complex iron-calcium cofactor catalyzing phosphotransfer chemistry.,  
920 *Science* (New York, N.Y.), 345, 1170–3, <https://doi.org/10.1126/science.1254237>, 2014.

921 Young, C. L. and Ingall, E. D.: Marine Dissolved Organic Phosphorus Composition: Insights from  
922 Samples Recovered Using Combined Electrodialysis/Reverse Osmosis, *Aquat Geochem*, 16, 563–574,  
923 <https://doi.org/10.1007/s10498-009-9087-y>, 2010.

924 Zhang, B., VerBerkmoes, N. C., Langston, M. A., Uberbacher, E., Hettich, R. L., and Samatova, N. F.:  
925 Detecting differential and correlated protein expression in label-free shotgun proteomics, *Journal of*  
926 *Proteome Research*, 5, 2909–2918, <https://doi.org/10.1021/pr0600273>, 2006.

927

**Page 14: [1] Deleted**

**Noelle Held**

**7/16/25 10:53:00 AM**

▼.....  
▲.....

**Page 17: [2] Deleted**

**Noelle Held**

**7/16/25 11:51:00 AM**

✖.....